Inorg. Chem. **2006**, *45*, 6864–6874

Phosphorus(I) Iodide: A Versatile Metathesis Reagent for the Synthesis of Low Oxidation State Phosphorus Compounds

Bobby D. Ellis and Charles L. B. Macdonald*

Department of Chemistry and Biochemistry, University of Windsor, Windsor, Ontario, Canada N9B 3P4

Received February 1, 2006

An improved method for the synthesis of cyclic low oxidation state P cations is presented. The only byproducts of the reaction of phosphorus triiodide with chelating phosphines are readily removed, resulting in an easily accessible P^I reagent with an anion that can be readily replaced through salt metathesis chemistry. These P^I salts are surprisingly stable, even in O_2 and moisture, and the origin of this unusual stability is elucidated using density functional theory calculations.

Introduction

The synthesis and examination of compounds containing P in low-coordinate bonding environments have been a focus of modern main group chemistry.[1,2] The observations and conclusions derived from such investigations, in conjunction with the realization of the close relationship between the behavior of P and C, have provided for an incredible advancement in the understanding of the structure, bonding, and reactivity of P compounds in particular and those of the p-block elements more generally.[3] The preceding studies of P compounds have typically concentrated on compounds containing the element in either of the common oxidation states (3+ or 5+).[4] Excluding metal phosphide minerals, the chemistry of compounds containing P in lower oxidation states has been largely limited to investigations of transient phosphinidenes, their transition-metal or Lewis-base adducts, their cyclic polyphosphine oligomers, other catenated polyphosphines, and elemental P.[1,2,5−8] The related chemistry of the heavier pnictogen (Pn) derivatives has been largely ignored.[9−11]

We required readily accessible and functionalizable low oxidation state group 15 reagents as a necessary starting point for our investigation of low oxidation state p-block chemistry; because of their relative stability in comparison to other P^I compounds, salts containing "triphosphenium" cations of the type first described by Schmidpeter and co-workers presented an ideal starting point.[12−15] These cations are related to phospha-Wittig reagents and other dicoordinate P compounds investigated by Schmidpeter and others, in which either one or both phosphines are replaced by anionic groups.[16−18] Furthermore, triphosphenium cations **1** are the heavier analogues of the ubiquitous and inert bis(triphosphoranylidene)ammonium ("PNP") cations **2** that are used as noncoordinating cations in numerous salts. Such cations are also isovalent with carbodiphosphoranes **3**, which are interesting ligands for transition metal complexes[19] and are

* To whom correspondence should be addressed. E-mail: cmacd@uwindsor.ca.

(1) Dillon, K. B.; Mathey, F.; Nixon, J. F. *Phosphorus: The Carbon Copy*; John Wiley & Sons: Chichester, U.K., 1998.
(2) Regitz, M., Scherer, O. J., Eds. *Multiple Bonds and Low Coordination in Phosphorus Chemistry*; Georg Thieme Verlag: Stuttgart, 1990.
(3) Bouhadir, G.; Bourissou, D. *Chem. Soc. Rev.* **2004**, *33*, 210−217.
(4) We prefer to use a simple, chemically intuitive convention in which the oxidation state of P is indicated by the number of lone pairs associated with the atom: P^{5+} has zero lone pairs, P^{3+} has one lone pair, and P^+ has two lone pairs.
(5) Baudler, M.; Glinka, K. *Chem. Rev.* **1993**, *93*, 1623−1667.
(6) Mathey, F. *Angew. Chem., Int. Ed. Engl.* **1987**, *26*, 275−286.
(7) Lammertsma, K.; Vlaar, M. J. M. *Eur. J. Org. Chem.* **2002**, 1127−1138.
(8) Lammertsma, K. *Top. Curr. Chem.* **2003**, *229*, 95−119.
(9) Driess, M.; Ackermann, H.; Aust, J.; Merz, K.; Von Wullen, C. *Angew. Chem., Int. Ed.* **2002**, *41*, 450−453.
(10) Barnham, R. J.; Deng, R. M. K.; Dillon, K. B.; Goeta, A. E.; Howard, J. A. K.; Puschmann, H. *Heteroat. Chem.* **2001**, *12*, 501−510.
(11) Dikarev, E. V.; Li, B. *Inorg. Chem.* **2004**, *43*, 3461−3466.
(12) Schmidpeter, A.; Lochschmidt, S.; Sheldrick, W. S. *Angew. Chem., Int. Ed. Engl.* **1982**, *21*, 63−64.
(13) Schmidpeter, A.; Lochschmidt, S. *Inorg. Synth.* **1990**, *27*, 253−258.
(14) Lochschmidt, S.; Schmidpeter, A. *Z. Naturforsch., B: Anorg. Chem., Org. Chem.* **1985**, *40B*, 765−773.
(15) Schmidpeter, A. *Heteroat. Chem.* **1999**, *10*, 529−537.
(16) Shah, S.; Protasiewicz, J. D. *Coord. Chem. Rev.* **2000**, *210*, 181−201.
(17) Schmidpeter, A.; Zwaschka, F. *Angew. Chem., Int. Ed. Engl.* **1977**, *16*, 704−705.
(18) Schmidpeter, A.; Burget, G.; Zwaschka, F.; Sheldrick, W. S. *Z. Anorg. Allg. Chem.* **1985**, *527*, 17−32.
(19) Schmidbaur, H. *Angew. Chem., Int. Ed. Engl.* **1983**, *22*, 907−927.

10.1021/ic060186o CCC: $33.50
Published on Web 07/19/2006

potential di-Wittig reagents for organic synthesis.[20]

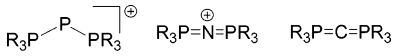

1 **2** **3**

The unique reactivity of P^I and As^I compounds is exemplified by Driess' synthesis of the first square-planar phosphonium and arsonium salts through the action of P^I and As^I sources on Schwartz's reagent.[9,21] Despite such unprecedented and impressive results, the behavior and utility of compounds such as **1** have not been explored or exploited to any significant extent. To successfully investigate many types of reactivities that may be exhibited by such salts, the presence of a robust and nonreactive counteranion is of critical importance. In this light, we required a suitable source for Pn^I ions in which we could readily change the counteranion. Thus, we recently reported the synthesis, characterization, and initial reactivity studies of new and valuable phosphorus(I) and arsenic(I) iodide salts.[22] Herein we detail the facile synthesis of the iodide salts of two stable P^I sources, [[1,2-bis(diphenylphosphino)ethane]phosphorus]$^+$ (**4**) and [[1,3-bis(diphenylphosphino)propane]phosphorus]$^+$ (**5**), and describe the metathesis reactivity of these reagents. In addition, the structural features, reactivities, and remarkable stabilities of selected examples of such compounds are explained using density functional theory (DFT) calculations.

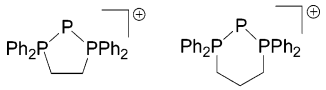

4 **5**

Experimental Section

Reagents and General Procedures. All manipulations were carried out using standard inert atmosphere techniques. Phosphorus(III) iodide, 1,2-bis(diphenylphosphino)ethane (dppe), 1,3-bis(diphenylphosphino)propane (dppp), silver trifluoromethanesulfonate (silver triflate, AgOTf), and potassium hexafluorophosphate were purchased from Strem Chemicals Inc., and all other chemicals and reagents were obtained from Aldrich; all reagents were used without further purification. MeOH was dried over Mg turnings, and all other solvents were dried on a series of Grubbs'-type columns[23] and were degassed prior to use. CD_2Cl_2 was dried over calcium hydride. Ag salts are sensitive to light, and precautions were taken to minimize light exposure in reactions involving such salts. The compound $dppeI_4$ (**6**) was synthesized by the slight modification of a literature procedure.[24] The relatively low yields of the iodide salts **4**[I] and **5**[I] are a consequence of the extensive washing with tetrahydrofuran (THF) used to remove the I_2; such treatment dissolves some of the iodide salt and also promotes the formation of an insoluble orange byproduct, which must be removed by filtration.

Instrumentation. NMR spectra were recorded at room temperature in CD_2Cl_2 solutions on a Bruker Avance 300-MHz spectrometer. Chemical shifts are reported in ppm, relative to external standards ($SiMe_4$ for ^1H and ^{13}C NMR, 85% aqueous H_3PO_4 for ^{31}P NMR, $BF_3{\cdot}OEt_2$ for ^{11}B NMR, $CFCl_3$ for ^{19}F NMR, and 0.05 M $Ga(NO_3)_3$ for ^{71}Ga NMR). Coupling constant magnitudes, $|J|$, are given in hertz. Melting points (Mp) or decomposition points (Dp) were obtained on samples sealed in glass capillaries under dry N_2 using an Electrothermal melting point apparatus. Elemental analysis was performed in-house using a PerkinElmer 2400 C, H, and N analyzer in the Centre for Catalysis and Materials Research, Department of Chemistry and Biochemistry, University of Windsor, Windsor, Ontario, Canada.

Theoretical Methods. Calculations were performed with the *Gaussian98* suite of programs.[25] Geometry optimizations have been calculated using DFT, specifically implementing the B3PW91 method [containing Becke's three-parameter hybrid functional for exchange (B3, including ca. 20% Hartree−Fock exchange)[26] combined with the generalized gradient approximation for correlation of Perdew and Wang (PW91)[27]] in conjunction with the 6-31+G(d) basis set. The geometries were restricted to the highest reasonable symmetry, and each stationary point was confirmed to be a minimum having zero imaginary vibrational frequencies. The electronic energies of the molecules have been corrected by the unscaled, zero-point vibrational energy (ZPVE). Single point energies have been calculated at the B3PW91/6-311+G(3df,2p)//B3PW91/6-31G(d) level of theory. Population analyses were conducted using the natural bond orbital (NBO)[28] method implemented in *Gaussian98*.

Preparation of [(dppe)P][I] (4[I]) from PI_3. A colorless solution of dppe (5.071 g, 12.728 mmol) in CH_2Cl_2 was added to a red solution of PI_3 (5.240 g, 12.728 mmol) in CH_2Cl_2 (100 mL), which resulted in the formation of a burgundy solution and an orange precipitate. Volatile components were removed under reduced pressure, and the crude residue was washed with THF (3×30 mL). The solid was redissolved in CH_2Cl_2 (75 mL) and filtered through Celite to remove further small amounts of orange precipitate. Volatiles were again removed in vacuo, and after dissolution in MeCN and slow evaporation of the solvent, a colorless crystalline material was obtained. Yield: 52% (3.680 g, 6.615 mmol). $^{31}P\{^1H\}$ NMR: −231.4 (t, $^1J_{PP} = 453$, 1P), 64.4 (d, $^1J_{PP} = 453$, 1P) [lit.[29] −232.7 (t, $^1J_{PP} = 453$), 62.9 (d, $^1J_{PP} = 453$)]. $^{13}C\{^1H\}$ NMR: 30.3 (d, $^1J_{CP} = 42$), 126.2 (dd, $^1J_{CP} = 75$, $^2J_{CP} = 8$), 130.2 (s), 133.0 (s), 134.0 (s). ^1H NMR: 3.54 (d, $^2J_{HP} = 16$, 4H), 7.58 (m, 12H), 7.87 (m, 8H). Dp: 149−150 °C. Anal. Calcd for $C_{26}H_{24}IP_3$ (556.295): C, 56.14; H, 4.35. Found: C, 54.92; H, 4.32.

(20) Schmidbaur, H. *Pure Appl. Chem.* **1978**, *50*, 19−25.
(21) Driess, M.; Aust, J.; Merz, K.; Van Wullen, C. *Angew. Chem., Int. Ed.* **1999**, *38*, 3677−3680.
(22) Ellis, B. D.; Carlesimo, M.; Macdonald, C. L. B. *Chem. Commun.* **2003**, 1946−1947.
(23) Pangborn, A. B.; Giardello, M. A.; Grubbs, R. H.; Rosen, R. K.; Timmers, F. J. *Organometallics* **1996**, *15*, 1518−1520.
(24) Schmidt, S. P.; Brooks, D. W. *Tetrahedron Lett.* **1987**, *28*, 767−768.
(25) Frisch, M. J.; Trucks, G. W.; Schlegel, H. B.; Scuseria, G. E.; Robb, M. A.; Cheeseman, J. R.; Zakrzewski, V. G.; Montgomery, V. G., Jr.; Stratmann, R. E.; Burant, J. C.; Dapprich, S.; Millam, J. M.; Daniels, A. D.; Kudin, K. N.; Strain, M. C.; Farkas, O.; Tomasi, J.; Barone, V.; Cossi, M.; Cammi, R.; Mennucci, B.; Pomelli, C.; Adamo, C.; Clifford, S.; Ochterski, J.; Petersson, G. A.; Ayala, P. Y.; Cui, Q.; Morokuma, K.; Salvador, P.; Dannenberg, J. J.; Malick, D. K.; Rabuck, A. D.; Raghavachari, K.; Foresman, J. B.; Cioslowski, J.; Ortiz, J. V.; Baboul, A. G.; Stefanov, B. B.; Liu, G.; Liashenko, A.; Piskorz, P.; Komaromi, I.; Gomperts, R.; Martin, R. L.; Fox, D. J.; Keith, T.; Al-Laham, M. A.; Peng, C. Y.; Nanayakkara, A.; Challacombe, M.; Gill, P. M. W.; Johnson, B.; Chen, W.; Wong, M. W.; Andres, J. L.; Gonzalez, C.; Head-Gordon, M.; Replogle, E. S.; Pople, J. A. *Gaussian 98*, revision A.11.1; Gaussian, Inc.: Pittsburgh, PA, 2001.
(26) Becke, A. D. *J. Chem. Phys.* **1993**, *98*, 5648−5652.
(27) Perdew, J. P.; Wang, Y. *Phys. Rev. B: Condens. Matter* **1992**, *45*, 13244−13249.
(28) Reed, A. E.; Curtiss, L. A.; Weinhold, F. *Chem. Rev.* **1988**, *88*, 899−926.
(29) Boon, J. A.; Byers, H. L.; Dillon, K. B.; Goeta, A. E.; Longbottom, D. A. *Heteroat. Chem.* **2000**, *11*, 226−231.

Preparation of 4[I] from P_2I_4. **4**[I] can also be prepared from P_2I_4 (0.796 g, 1.398 mmol) and dppe (1.114 g, 2.795 mmol) in a 1:2 ratio in a manner similar to the preparation from PI_3. Yield: 39% (0.603 g, 1.084 mmol). Identical spectroscopic data are observed as when **4**[I] is prepared from PI_3.

Preparation of [(dppp)P][I] (5[I]) from PI_3. A colorless solution of dppp (3.247 g, 7.872 mmol) in CH_2Cl_2 was added to a red solution of PI_3 (3.241 g, 7.872 mmol) in CH_2Cl_2 (100 mL), which produced a reddish-orange solution and an orange precipitate. The volatile components were removed under reduced pressure, and the crude residue was washed with THF (3 × 30 mL). The solid was redissolved in CH_2Cl_2 (75 mL) and filtered through Celite to remove further small amounts of orange precipitate. The solvent was again removed in vacuo, and after dissolution in MeCN and slow evaporation of the solvent, a colorless crystalline material was obtained. Yield: 56% (2.531 g, 4.438 mmol). $^{31}P\{^1H\}$ NMR: −209.5 (t, $^1J_{PP}$ = 423, 1P), 22.4 (d, $^1J_{PP}$ = 423, 2P) [lit.[29] −208.9 (t, $^1J_{PP}$ = 423), 23.5 (d, $^1J_{PP}$ = 423)]. $^{13}C\{^1H\}$ NMR: 19.5 (s), 25.0 (d, $^1J_{CP}$ = 47), 125.7 (dd, $^1J_{CP}$ = 77, $^2J_{CP}$ = 12), 130.2 (s), 132.4 (s), 134.0 (s). ^1H NMR: 2.56 (m, 2H), 3.05 (m, 4H), 7.44 (m, 8H), 7.65 (m, 12H). Dp: 96−97 °C. Anal. Calcd for $C_{27}H_{26}IP_3$ (570.321): C, 56.86; H, 4.60. Found: C, 56.32; H, 4.99.

Preparation of 5[I] from P_2I_4. **5**[I] can also be prepared from P_2I_4 (0.454 g, 0.797 mmol) and dppp (0.658 g, 1.594 mmol) in a 1:2 ratio in a manner similar to the preparation from PI_3. Yield: 17% (0.156 g, 0.274 mmol). Identical spectroscopic data are observed as when **5**[I] is prepared from PI_3.

Preparation of [(dppe)P][BPh_4] (4[BPh_4]). To a colorless solution of **4**[I] (0.625 g, 1.124 mmol) in MeOH (10 mL) was added a colorless solution of [Na][BPh_4] (0.384 g, 1.124 mmol) in MeOH (10 mL), and a white precipitate formed instantly. The precipitate was collected by filtration and washed with MeOH (5 mL). The crude product was dissolved in MeCN, and upon slow evaporation of the solvent, a colorless crystalline material was deposited. Yield: 98% (0.824 g, 1.100 mmol). $^{31}P\{^1H\}$ NMR: −235.5 (t, $^1J_{PP}$ = 456, 1P), 64.4 (d, $^1J_{PP}$ = 456, 2P). $^{11}B\{^1H\}$ NMR: −6.9 (s). $^{13}C\{^1H\}$ NMR: 29.0 (d, $^1J_{CP}$ = 46), 122.4 (s), 125.9 (dd, $^1J_{CP}$ = 75, $^2J_{CP}$ = 9), 126.2 (s), 130.2 (s), 132.8 (s), 134.2 (s), 136.4 (s), 164.4 (q, $^1J_{CB}$ = 49). ^1H NMR: 2.48 (d, $^2J_{HP}$ = 16, 4H), 6.80 (m, 4H), 6.93 (m, 8H), 7.33 (m, 8H), 7.60 (m, 20H). Mp: 174−175 °C. Anal. Calcd for $C_{50}H_{44}BP_3$ (748.617): C, 80.22; H, 5.92. Found: C, 77.83; H, 6.68.

Preparation of [(dppp)P][BPh_4] (5[BPh_4]). To a colorless solution of **5**[I] (0.225 g, 0.395 mmol) in MeOH (10 mL) was added a colorless solution of [Na][BPh_4] (0.135 g, 0.395 mmol) in MeOH (10 mL), and a white precipitate formed instantly. The precipitate was collected by filtration and washed with MeOH (5 mL). The crude product was dissolved in MeCN, and upon slow evaporation of the solvent, a colorless crystalline material formed. Yield: 71% (0.214 g, 0.281 mmol). $^{31}P\{^1H\}$ NMR: −210.2 (t, $^1J_{PP}$ = 424, 1P), 22.7 (d, $^1J_{PP}$ = 424, 2P). $^{11}B\{^1H\}$ NMR: −6.9 (s). $^{13}C\{^1H\}$ NMR: 19.1 (s), 25.2 (d, $^1J_{CP}$ = 47), 122.4 (s), 125.6 (dd, $^1J_{CP}$ = 75, $^2J_{CP}$ = 9), 126.2 (s), 130.2 (s), 132.3 (s), 134.0 (s), 136.5 (s), 164.6 (q, $^1J_{CB}$ = 49). ^1H NMR: 2.06 (m, 2H), 2.44 (m, 4H), 6.89 (m, 4H), 7.02 (m, 8H), 7.36 (m, 8H), 7.52 (m, 20H). Mp: 168−169 °C. Anal. Calcd for $C_{51}H_{46}BP_3$ (762.643): C, 80.32; H, 6.08. Found: C, 79.66; H, 6.39.

Preparation of [(dppp)P][OTf] (5[OTf]). To a colorless solution of **5**[I] (0.176 g, 0.309 mmol) in MeOH (10 mL) was added a colorless solution of [Ag][OTf] (0.079 g, 0.309 mmol) in MeOH (10 mL), and a yellow precipitate formed instantly. The volatile components were removed under reduced pressure, and the product was extracted from the crude reaction mixture using CH_2Cl_2 (15 mL) followed by filtration through Celite. Slow evaporation of the solvent afforded a colorless crystalline material. Yield: 69% (0.126 g, 0.213 mmol). $^{31}P\{^1H\}$ NMR: −210.0 (t, $^1J_{PP}$ = 424, 1P), 22.7 (d, $^1J_{PP}$ = 424, 2P). $^{19}F\{^1H\}$ NMR: −79.1 (s). $^{13}C\{^1H\}$ NMR: 19.4 (s), 25.5 (d, $^1J_{CP}$ = 48), 121.7 (q, $^1J_{CF}$ = 321), 126.0 (dd, $^1J_{CP}$ = 76, $^2J_{CP}$ = 11), 130.2 (s), 132.6 (s), 133.9 (s). ^1H NMR: 2.57 (m, 2H), 3.04 (m, 4H), 7.47 (m, 8H), 7.65 (m, 12H). Dp: 177−178 °C. Anal. Calcd for $C_{28}H_{26}F_3O_3P_3S\cdot CH_2Cl_2$ (677.419): C, 51.42; H, 4.17. Found: C, 52.23; H, 4.54. Crystallographic experiments on crystals of **5**[OTf] yielded data of relatively low quality; while the identities and connectivities of the component ions are confirmed, the metrical parameters are unreliable. Please refer to the Supporting Information for details.

Preparation of [(dppp)P][PF_6] (5[PF_6]). To a colorless solution of **5**[I] (0.509 g, 0.892 mmol) in MeOH (10 mL) was added a colorless solution of [K][PF_6] (0.164 g, 0.892 mmol) in MeOH (10 mL), and the mixture became slightly cloudy white. The mixture was stirred for 30 min. The volatile components were removed under reduced pressure, and the product was extracted from the crude reaction mixture using CH_2Cl_2 (15 mL) followed by filtration through Celite. Slow evaporation of the solvent produced a colorless crystalline material. Yield: 53% (0.277 g, 0.471 mmol). $^{31}P\{^1H\}$ NMR: −210.2 (t, $^1J_{PP}$ = 424, 1P), −143.8 (sept, $^1J_{PF}$ = 711, 1P), 22.6 (d, $^1J_{PP}$ = 424, 2P). $^{19}F\{^1H\}$ NMR: −73.4 (d, $^1J_{FP}$ = 711). $^{13}C\{^1H\}$ NMR: 19.4 (s), 25.6 (d, $^1J_{CP}$ = 48), 125.8 (dd, $^1J_{CP}$ = 76, $^2J_{CP}$ = 11), 130.2 (s), 132.5 (s), 134.0 (s). ^1H NMR: 2.60 (m, 2H), 2.99 (m, 4H), 7.49 (m, 8H), 7.67 (m, 12H). Mp: 185−186 °C. Anal. Calcd for $C_{27}H_{26}F_6P_4$ (588.381): C, 55.12; H, 4.45. Found: C, 54.96; H, 4.71.

Preparation of [(dppp)P][$GaCl_4$] (5[$GaCl_4$]). To a colorless solution of **5**[I] (0.369 g, 0.647 mmol) in MeOH (10 mL) was added a colorless solution of [Li][$GaCl_4$] (0.141 g, 0.647 mmol) in MeOH (10 mL), and the mixture became slightly cloudy white. The mixture was stirred for 30 min. The volatile components were removed under reduced pressure, and the product was extracted from the crude reaction mixture using CH_2Cl_2 (15 mL) followed by filtration through Celite. Slow evaporation of the solvent yielded a colorless crystalline material. Yield: 31% (0.130 g, 0.198 mmol). $^{31}P\{^1H\}$ NMR: −209.9 (t, $^1J_{PP}$ = 425, 1P), 22.6 (d, $^1J_{PP}$ = 425, 2P). ^{71}Ga NMR: 249 (s). $^{13}C\{^1H\}$ NMR: 19.6 (s), 25.9 (d, $^1J_{CP}$ = 47), 125.6 (dd, $^1J_{CP}$ = 76, $^2J_{CP}$ = 11), 130.3 (s), 132.5 (s), 134.1 (s). ^1H NMR: 2.60 (m, 2H), 2.98 (m, 4H), 7.50 (m, 8H), 7.64 (m, 12H). Mp: 195−196 °C. Anal. Calcd for $C_{27}H_{26}Cl_4GaP_3$ (654.950): C, 49.51; H, 4.00. Found: C, 49.56; H, 4.22.

Preparation of [(dppp)P][BF_4] (5[BF_4]). To a colorless solution of **5**[I] (0.183 g, 0.321 mmol) in MeOH (10 mL) was added a colorless solution of [Na][BF_4] (0.035 g, 0.321 mmol) in MeOH (10 mL), with no noticeable color change. The mixture was stirred for 30 min. The volatile components were removed under reduced pressure, and the product was extracted from the crude reaction mixture using CH_2Cl_2 (15 mL) followed by filtration through Celite. Slow evaporation of the solvent afforded a colorless crystalline material. Yield: 66% (0.113 g, 0.213 mmol). $^{31}P\{^1H\}$ NMR: −209.7 (t, $^1J_{PP}$ = 423, 1P), 22.7 (d, $^1J_{PP}$ = 423, 2P). $^{11}B\{^1H\}$ NMR: −1.3 (s). $^{19}F\{^1H\}$ NMR: −152.9 (s). $^{13}C\{^1H\}$ NMR: 19.6 (s), 25.4 (d, $^1J_{CP}$ = 48), 125.9 (dd, $^1J_{CP}$ = 77, $^2J_{CP}$ = 10), 130.1 (s), 132.6 (s), 133.8 (s). ^1H NMR: 2.59 (m, 2H), 3.14 (m, 4H), 7.47 (m, 8H), 7.65 (m, 12H). The results of several single-crystal diffraction experiments suggest that the crystals contain a mixture of [BF_4] and [I] anions; thus, microanalysis experiments were not undertaken. Please refer to the Supporting Information for details.

X-ray Crystallography. Crystals were coated in Nujol, Fluoro-Lube, or Paratone-N, mounted on a glass fiber, and placed in the

Table 1. Summary of X-ray Crystallographic Data for Compounds **4**[I], **4**[BPh_4], **5**[I], **5**[BPh_4], **5**[PF_6], **5**[$GaCl_4$], and **6**

compd	**4[I]**	**5[I]**	**4[BPh_4]**	**5[BPh_4]**	**5[PF_6]**	**5[$GaCl_4$]**	**6**
empirical formula	$C_{26}H_{24}IP_3$	$C_{27}H_{26}IP_3$	$C_{50}H_{44}BP_3$	$C_{51}H_{46}BP_3$	$C_{27}H_{26}F_6P_4$	$C_{27}H_{26}Cl_4GaP_3$	$C_{26}H_{24}I_4P_2$
fw	556.26	570.29	748.22	762.60	588.36	654.91	905.99
T (K)	173(2)	173(2)	173(2)	173(2)	173(2)	173(2)	173(2)
wavelength (Å)	0.710 73	0.710 73	0.710 73	0.710 73	0.710 73	0.710 73	0.710 73
cryst syst	triclinic	monoclinic	monoclinic	monoclinic	monoclinic	monoclinic	orthorhombic
space group	$P\bar{1}$	$P2_1/c$	$P2_1/n$	$P2_1/c$	$P2_1/c$	$P2_1/c$	$Aba2$
unit cell dimens							
a (Å)	10.1179(13)	10.9315(10)	12.0031(8)	12.244(3)	12.690(8)	9.7274(16)	15.2158(8)
b (Å)	13.5649(17)	19.2143(18)	17.5742(12)	17.883(3)	15.736(9)	14.815(3)	15.2876(8)
c (Å)	19.688(3)	12.9085(12)	19.6302(13)	21.258(4)	17.815(8)	21.255(3)	12.3342(6)
α (deg)	71.970(1)	90	90	90	90	90	90
β (deg)	81.280(1)	110.931(2)	100.893(1)	114.957(10)	131.57(3)	106.894(6)	90
γ (deg)	68.866(1)	90	90	90	90	90	90
V (Å^3)	2394.2(5)	2532.4(4)	4066.3(5)	4220.0(15)	2662(3)	2930.9(9)	2869.1(3)
Z	4	4	4	4	4	4	4
D_{calcd} (g cm^{-3})	1.543	1.496	1.223	1.200	1.468	1.484	2.097
abs coeff (mm^{-1})	1.549	1.467	0.181	0.176	0.342	1.483	4.469
F(000)	1112	1144	1576	1608	1208	1328	1688
θ range for data collection (deg)	1.09−27.50	1.99−27.49	1.57−27.50	1.55−27.50	2.00−27.50	1.70−27.50	2.51−27.49
limiting indices	$-13 \le h \le 13$ $-17 \le k \le 17$ $-25 \le l \le 25$	$-13 \le h \le 14$ $-24 \le k \le 24$ $-16 \le l \le 16$	$-15 \le h \le 15$ $-22 \le k \le 22$ $-25 \le l \le 25$	$-15 \le h \le 14$ $-20 \le k \le 23$ $-27 \le l \le 27$	$-16 \le h \le 16$ $-20 \le k \le 19$ $-22 \le l \le 21$	$-12 \le h \le 12$ $-19 \le k \le 19$ $-26 \le l \le 26$	$-19 \le h \le 19$ $-19 \le k \le 19$ $-15 \le l \le 15$
reflns colld	26 843	24 349	39 288	29 565	21 301	40 601	13 423
indep reflns	10 586	5809	9355	9692	5693	6663	3294
R_{int}	0.0330	0.0229	0.0350	0.1148	0.0654	0.0442	0.0245
data/restraints/param	10586/0/585	5809/0/280	9355/0/529	9692/0/496	5693/0/334	6663/0/316	3294/1/163
GOF on F^2	1.299	1.033	1.011	0.962	1.199	1.148	1.055
final R indices[a] [$I > 2\sigma(I)$]	R1 = 0.0596	R1 = 0.0206	R1 = 0.0435	R1 = 0.0626	R1 = 0.0938	R1 = 0.0505	R1 = 0.0195
	wR2 = 0.1177	wR2 = 0.0507	wR2 = 0.1121	wR2 = 0.1008	wR2 = 0.2195	wR2 = 0.1010	wR2 = 0.0469
R indices (all data)	R1 = 0.0694	R1 = 0.0241	R1 = 0.0578	R1 = 0.2144	R1 = 0.1231	R1 = 0.0691	R1 = 0.0202
	wR2 = 0.1240	wR2 = 0.0522	wR2 = 0.1238	wR2 = 0.1460	wR2 = 0.2299	wR2 = 0.1115	wR2 = 0.0473
largest difference map peak and hole (e Å^{-3})	1.348, −0.914	0.653, −0.253	0.402, −0.260	0.263, −0.202	0.629, −0.5	0.588, −0.294	0.857, −0.360

N_2 boil-off stream of the Kryoflex low-temperature apparatus. Reflection data were integrated from frame data obtained using a hemisphere of scans on a Bruker APEX CCD diffractometer using Mo Kα radiation (λ = 0.710 73 Å). Diffraction data and unit cell parameters were consistent with the assigned space groups. Lorentz and polarization corrections and empirical absorption corrections, based on redundant data at varying effective azimuthal angles, were applied to the data sets using *SAINTPlus*[30] and *SADABS*[31] software. The structures were solved by direct methods using *SHELXS*[32] or *SIR97*[33] (as implemented in the WinGX package[34]), completed by subsequent Fourier syntheses, and refined with full-matrix least-squares methods against F^2 data using *SHELXL*.[35] All non-H atoms were refined anisotropically, and all H atoms were placed in appropriate geometrically calculated positions. Thermal ellipsoid plots of the molecular structures were generated using *SHELXTL*.[36] The experimental details for each of the diffraction experiments are listed in Table 1.

Results and Discussion

Syntheses of 4[I] and 5[I]. In the 1980s, Schmidpeter and co-workers reported the synthesis of a variety of triphosphenium salts **1** through the reduction of PCl_3 in the presence of trihydrocarbylphosphines or trisamidophosphines. The reducing agents used in these reactions were either $SnCl_2$ or an excess amount of the phosphine ligands (vide infra), and the resultant salts, containing anions such as $[SnCl_6]^{2-}$, $[AlCl_4]^-$, and $[BPh_4]^-$, were separated by fractional crystallization from the byproducts.[12,37,38] Some of the byproducts, such as $[ClP(NMe_2)_3][BPh_4]$, have solubility characteristics very similar to those of the desired salts; thus, the isolation of high-purity triphosphenium salts is difficult, and the yields are relatively small using this approach.

While the triphosphenium cations appear to be a reasonable source of P^I centers, some of the anions obtained using Schmidpeter's original methods are not suitable for many of the reactivity studies that we wish to pursue. For example, salt containing tetrachloroaluminate anions may be susceptible to degradation by nucleophiles, the salts containing such metalate anions may also be air- or moisture-sensitive, and the insolubility of certain triphosphenium salts could hinder our investigations. For this reason, we sought a convenient and relatively high-yield synthesis of pnictogen(I) halides with the hope that such compounds would be useful reagents for the metathetical preparation of salts with any desired counteranion.

(30) *SAINTPlus*; Bruker AXS Inc.: Madison, WI, 2001.
(31) *SADABS*; Bruker AXS Inc.: Madison, WI, 2001.
(32) Sheldrick, G. M. *SHELXS-97*; Universitat Gottingen: Gottingen, Germany, 1997.
(33) Altomare, A.; Burla, M. C.; Camalli, M.; Cascarano, G.; Giacovazzo, C.; Guagliardi, A.; Polidori, G.; Spagna, R. *SIR97*; CNR−IRMEC: Bari, 1997.
(34) Farrugia, L. J. *J. Appl. Crystallogr.* **1999**, *32*, 837−838.
(35) Sheldrick, G. M. *SHELXL-97*; Universitat Gottingen: Gottingen, Germany, 1997.
(36) Sheldrick, G. M. *SHELXTL*; Bruker AXS Inc.: Madison, WI, 2001.
(37) Schmidpeter, A.; Lochschmidt, S.; Sheldrick, W. S. *Angew. Chem., Int. Ed. Engl.* **1985**, *24*, 226−227.
(38) Schmidpeter, A.; Lochschmidt, S. *Angew. Chem., Int. Ed. Engl.* **1986**, *25*, 253−254.

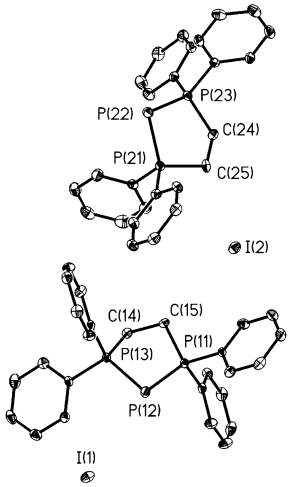

Figure 1. Thermal ellipsoid plot (30% probability surface) of **4**[I]. H atoms are omitted for clarity.

Because the reduction of PI_3 should be easier than that of any of the lighter phosphorus trihalides, we chose to concentrate on the generation of iodide salts. In this vein, the room-temperature reaction of PI_3 with dppe in dichloromethane (eq 1) rapidly produces a burgundy solution. *It*

$$PI_3 \xrightarrow[-I_2]{\text{dppe or dppp}} \underset{\mathbf{4}[I]}{[(dppe)P][I]} \text{ or } \underset{\mathbf{5}[I]}{[(dppp)P][I]} \qquad (1)$$

is important to note that the use of the non-nucleophilic solvent is necessary to avoid excessive formation of byproducts. After 2 h of stirring, the volatile components were removed under reduced pressure and the solid was washed rapidly with THF to remove the resultant I_2.[39] It must be noted that while the formation of the cation is quantitative according to ^{31}P NMR spectra of the reaction mixture, the concentration of the reaction mixture and, particularly, the washing of the crude solid with THF to remove the I_2 results in the formation of an orange byproduct and reduces the isolated yield. Redissolution of the crude solid in dichloromethane and filtration to remove any of the insoluble orange byproduct affords pale yellow solutions that deposit colorless solid upon concentration. Multinuclear NMR spectra of the solid exhibit signals that are attributable to the cation $[(dppe)P]^+$ **4**. Negative-ion electrospray mass spectrometry experiments and microanalytical data for the product are consistent with the proposed composition as an iodide salt and not a triiodide salt. It should be noted that **4**[I] is stable in air and can be washed with water in the open atmosphere.

The proposed composition of the salt is also supported by the results of an X-ray crystallographic investigation. Whereas the precipitated salts of **4**[I] are generally microcrystalline materials that are unsuitable for single-crystal diffraction studies, larger crystals of **4**[I] may be obtained by recrystallization from MeCN. The salt crystallizes in the space group $P\bar{1}$ with two independent ion pairs in the asymmetric unit, as illustrated in Figure 1. One notable feature of the structure is the lack of any close interactions between the cations and anions; the shortest P−I distance is 4.702(3) Å, and the closest contacts to the I anions are, in fact, from various H atoms on the dppe ligands; these contacts are all in excess of 3.055(2) Å. The metrical parameters of the cation, listed in Table 2, are similar to those that have been observed in Schmidpeter's original hexachlorostannate salt of the $[(dppe)P]^+$ cation, $\mathbf{4}_2[SnCl_6]$.[12] For the cation containing P(11), the P−P distances of 2.1305(17) and 2.1260(17) Å [the corresponding values for the cation containing P(21) are 2.1328(17) and 2.1286(16) Å] compare well with the average distance of 2.133 Å found between dicoordinate and tetracoordinate P atoms in organophosphorus compounds reported in the Cambridge Structural Database (CSD).[40] It is noteworthy that these distances are significantly shorter than typical P−P single-bond lengths such as those found in Me_2P-PMe_2 [2.212(1) Å][41] or Ph_2P-PPh_2 [2.217(1) Å],[42] and they are likewise considerably shorter than the average distance of 2.215 Å between tricoordinate and tetracoordinate P atoms for organophosphorus compounds in the CSD.[40] The unusual shortness of the P−P bonds in cations such as **4**, even when differences in the covalent radii and coordination number are taken into account, is generally attributed to the presence of partial multiple bonding; the nature of the bonding in such cations is discussed in more detail in the Theoretical Results and Predictions section. The angle at the dicoordinate P atom 89.35(6)° [88.45(6)°] is notably small because of the geometric constraints of the dppe chelate.

In a similar manner, the room temperature reaction of PI_3 with dppp in dichloromethane also produces a reddish-orange solution with orange precipitate. Following stirring for 2 h and removal of the solvent, the crude product can be rinsed with THF to remove I_2. Extraction in dichloromethane affords colorless solutions that yield a colorless solid upon concentration. Signals in the multinuclear NMR spectra of the solid are attributable to the cation $[(dppp)P]^+$ **5**. The microcrystalline solid is air- and moisture-stable and can be recrystallized from MeCN to obtain material suitable for single-crystal X-ray diffraction. The salt crystallizes in the space group $P2_1/c$, the molecular structure is shown in Figure 2, and relevant metrical parameters are listed in Table 2. As observed in **4**[I], the P−P bond distances in **5**[I] are shorter than the typical single bonds and are similar to those observed in the only two other salts containing cations of this type, namely, $\mathbf{5}_2[SnCl_6]$ and $\mathbf{5}[AlCl_4]$.[29,43] The P−P−P angle of 97.77(2)° is wider than the corresponding angle in **4**[I] as one would expect for the six-membered ring produced by the larger and more flexible dppp chelate.

While the production of P^I derivatives from the direct reaction of phosphorus trihalides with various phosphine donors has been demonstrated unambiguously using ^{31}P

(39) EI-MS. Calcd for I_2 $[M]^+$: *m*/*z* 253.81. Found: *m*/*z* 253.61.

(40) Allen, F. H. *Acta Crystallogr., Sect. B: Struct. Sci.* **2002**, *B58*, 380−388.
(41) Mundt, O.; Riffel, H.; Becker, G.; Simon, A. *Z. Naturforsch., B: Chem. Sci.* **1988**, *43*, 952−958.
(42) Dashti-Mommertz, A.; Neumuller, B. *Z. Anorg. Allg. Chem.* **1999**, *625*, 954−960.
(43) Deng, R. M. K.; Goeta, A. E.; Dillon, K. B.; Thompson, A. L. *Acta Crystallogr., Sect. E: Struct. Rep. Online* **2005**, *E61*, m296−m298.

Table 2. Selected Metrical Parameters for Compounds **4**[I], **4**[BPh_4], **5**[I], **5**[BPh_4], **5**[PF_6], and **5**[$GaCl_4$]

	4[I]	**5**[I]	**4**[BPh_4]	**5**[BPh_4]	**5**[PF_6]	**5**[$GaCl_4$]
P(1)−P(2)	2.1263(17) [2.1223(18)]	2.1318(6)	2.1166(6)	2.1224(13)	2.122(2)	2.1276(12)
P(2)−P(3)	2.1315(18) [2.1240(18)]	2.1203(6)	2.1293(6)	2.1326(14)	2.113(2)	2.1211(12)
P(1)−C(5) [or −C(6)]	1.821(5) [1.820(5)]	1.8068(16)	1.8164(17)	1.807(3)	1.811(6)	1.815(3)
P(3)−C(4)	1.826(5) [1.837(5)]	1.8112(16)	1.8430(16)	1.804(3)	1.815(6)	1.816(3)
C(4)−C(5)	1.520(7) [1.500(7)]	1.533(2)	1.521(2)	1.523(4)	1.521(9)	1.532(5)
C(5)−C(6)		1.531(2)		1.523(4)	1.526(9)	1.530(4)
P(1)−P(2)−P(3)	88.37(7) [89.46(7)]	97.77(2)	86.52(2)	93.98(5)	97.19(9)	93.76(5)

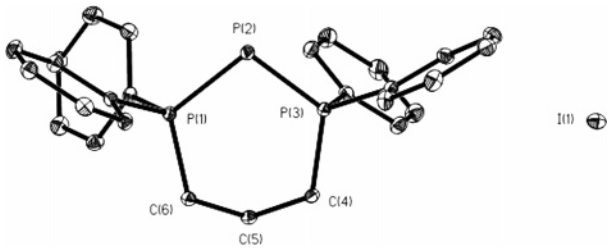

Figure 2. Thermal ellipsoid plot (30% probability surface) of **5**[I]. H atoms are omitted for clarity.

NMR methods,[29] the fact that these reactions proceed in such a manner is surprising in terms of both the known chemistry of P and that of its heavier congeners. For example, the reaction of equimolar amounts of PMe_3 and PBr_3 results in the formation of the Lewis acid−base adduct $Me_3P \rightarrow PBr_3$,[42] which is perhaps a more predictable result.[44] Similarly, the reaction of arsenic trihalides with mono- and bidentate phosphine or arsine donors also results in the formation of acid−base adducts in certain cases[45] or in the formation of the arsenic analogues of **1** in other instances.[10,46,47] In this light, the rapid and spontaneous nature of the reactions of PI_3 with the chelating donors outlined above is perhaps unexpected and is certainly dependent on the stoichiometries and conditions used for the reaction.

In 1985, Schmidpeter and associates demonstrated that the acyclic triphosphenium salt $[(Ph_3P)_2P][AlCl_4]$ is obtained by the reaction of PCl_3 with 3 equiv of PPh_3 in the presence of $AlCl_3$; the byproduct isolated from the reaction was $[ClPPh_3][AlCl_4]$, which indicates that 1 equiv of PPh_3 is oxidized during the course of the reaction.[37] Likewise, in 1986, the same researchers showed that the reaction of PCl_3 with 3 equiv of $P(NMe_2)_3$ in the presence of $[Na][BPh_4]$ proceeds in a similar manner to yield $[((Me_2N)_3P)_2P][BPh_4]$ and $[ClP(NMe_2)_3][BPh_4]$.[38] More recently, the spectroscopic investigations of Dillon and associates illustrated the spontaneous nature of the reduction of PX_3 (X = Cl, Br, I) to P^I cations in the absence of auxiliary reducing agents.[29] In each of these cases, the completely reasonable suggestion has been that a phosphine ligand acts as the redox couple for the reduction of P^{III} to P^I in that it is oxidized to the corresponding halophosphonium halide (P^{III} to P^V).

While a P^{III} to P^V redox couple is certainly plausible, the ^{31}P NMR spectra of the reaction mixtures described in this work do not show signals attributable to the iodophosphonium salt during the reaction of PI_3 with either of the chelating ligands *when the reactions are conducted in dichloromethane*. Under such conditions, significant amounts of iodophosphonium iodide byproducts are only observed if the initial reaction mixtures are allowed to stir for extended periods. In contrast, significant amounts of the iodophosphonium byproduct are generated when the reactions are performed in donor solvents such as THF or Et_2O. Given the foregoing, we believe that the experimental observations suggest that the iodophosphonium iodide byproduct is attributable to the reaction of 2 equiv of I_2 and dppe.[48] In this vein, we have verified that the reaction of 2 equiv of I_2 with dppe occurs in dichloromethane and produces color changes that are consistent with those observed after the formation of **4**[I] in reactions containing excess dppe. To confirm the NMR assignment, a mixture of dppe and 2 equiv of I_2 was concentrated to obtain yellow crystals that were suitable for analysis by single-crystal X-ray diffraction; the molecular structure of **6** is depicted in Figure 3.

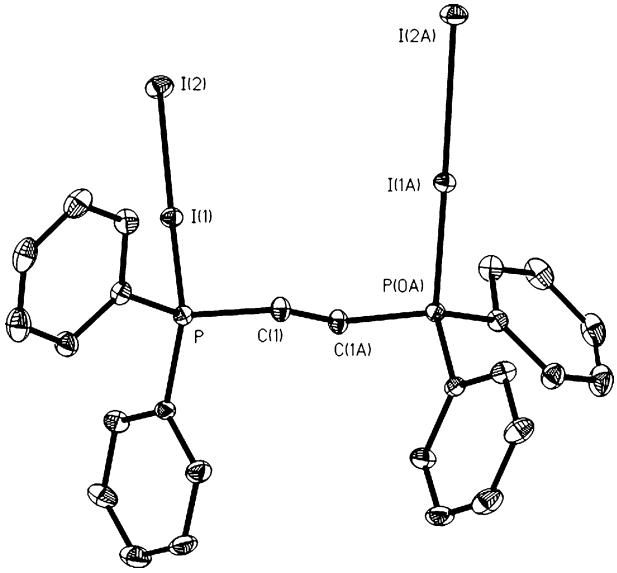

Figure 3. Thermal ellipsoid plot (30% probability surface) of **6**. H atoms are omitted for clarity.

The $dppeI_4$ complex crystallizes in the space group *Aba*2, and the individual molecules are linked to one another through a series of long (>3.0 Å) H−I intermolecular H bonds. The metrical parameters of the individual adducts are similar to those of other phosphine−iodine adducts. For example, the P−I bond length of 2.4712(1) Å and the I−I

(44) Burford, N.; Ragogna, P. J. *J. Chem. Soc., Dalton Trans.* **2002**, 4307−4315.
(45) Hill, N. J.; Levason, W.; Reid, G. *J. Chem. Soc., Dalton Trans.* **2002**, 1188−1192.
(46) Gamper, S. F.; Schmidbaur, H. *Chem. Ber.* **1993**, *126*, 601−604.
(47) Ellis, B. D.; Macdonald, C. L. B. *Inorg. Chem.* **2004**, *43*, 5981−5986.
(48) Godfrey, S. M.; Kelly, D. G.; McAuliffe, C. A.; Mackie, A. G.; Pritchard, R. G.; Watson, S. M. *J. Chem. Soc., Chem. Commun.* **1991**, 1163−1164.

distance of 3.1482(4) Å in **6** are comparable to the corresponding P−I [2.481(4) Å] and I−I [3.16(2) Å] distances found for Ph_3P-I_2.[48] While the structural features of the new adduct are unexceptional, the crystallographic investigation confirms the composition of **6**, which is a material that is soluble in dichloromethane and that produces a signal at 51 ppm in the $^{31}P\{^1H\}$ NMR spectrum. Most importantly, this result confirms that **6** is not formed in the preparations of **4**[I] or **5**[I] using the procedures described above.

Given the preceding observations and arguments, it is possible that the experimental observation of byproducts of the form $[X-PR_3]^+$ (X = Cl, Br) in the reduction of PX_3 results from the transient in situ formation of X_2. However, because Cl_2 and Br_2 are much more potent oxidizing agents than I_2 and will react more rapidly with PR_3 to form cations with stronger P−X bonds, it is unlikely that the intermediate formation of X_2 would be observed experimentally under conditions similar to those used for the synthesis of **4**[I]. In any event, in terms of being able to separate the P^I salt from the byproducts, the use of PI_3 as the P source in such preparative experiments allows one to obtain both greater yields and products of higher purity.

It is worth noting that insight into the mechanism of the formation of phosphorus(I) iodide in the process outlined in eq 1 is provided by the solution behavior of the phosphorus triiodide starting material itself. Variable-temperature ^{31}P NMR experiments reveal that, in solution, PI_3 is in equilibrium with P_2I_4 and I_2. We postulate that a further disproportionation to oligomeric $(P-I)_n$ may occur to provide the "P−I" fragments that are complexed by the dppe or dppp chelates. In accord with the results of previous investigations of the interaction of Lewis bases with halophosphines, this additional disproportionation is undoubtedly facilitated or enabled by the presence of the chelating ligands.[49] While we have, as yet, only obtained circumstantial evidence for the formation of $(P-I)_n$,[50] the existence of $(P-Cl)_6$ and $(P-Br)_6$ at low temperature has been reported,[51] and our investigations of the As analogue of **4**[I] reveal that the oxidative cleavage of the dppe ligand produces an ion containing an $(As-I)_6$ ring from the formal release of "As−I" fragments.[47] Regardless of the intermediacy of $(P-I)_n$, we have verified that the reaction of P_2I_4 with appropriate amounts of either dppe or dppp yields **4**[I] or **5**[I] with the concomitant elimination of I_2.

Anion Exchange. As anticipated, the I^- anion in **4**[I] or **5**[I] is readily replaced using metathesis reactions with a variety of alkali-metal or Ag salts. As depicted in eq 2, the reactions of **4**[I] or **5**[I] with [Na][BPh_4], [Ag][OTf], [K][PF_6], [Li][$GaCl_4$], or other suitable salts in methanol proceed rapidly at room temperature to produce the desired tetraphenylborate, triflate, hexafluorophosphate, or tetrachlorogallate salts, respectively. It must be noted that the use of solvents

[M][A] = [Na][BPh_4], [Ag][OTf], [K][PF_6], [Li][$GaCl_4$], [Na][BF_4], etc

other than methanol for such reactions generally gives products in significantly lower yield and of lower purity. Following extraction into dichloromethane, the colorless solution of the desired salt is filtered from the metal iodide byproduct and subsequent removal of all volatile compounds under reduced pressure provides colorless solid salts in high yield.

NMR studies of the salts demonstrate the integrity of either the $[(dppe)P]^+$ or the $[(dppp)P]^+$ cation in every case and suggest that there is little interaction between the anions and cations in solution. Although, in some instances, there are minor changes in the chemical shift of the P^I center depending on the identity of the anion in the salt, the differences from the chemical shift observed for the iodide salt are small in any case. Interestingly, salts containing air-stable counteranions such as tetraphenylborate or triflate appear to be stable for at least several hours upon exposure to air either as solids or as solutions in CD_2Cl_2. It should be emphasized that this behavior is in stark contrast to other P^I compounds (e.g., phosphinidenes) or dicoordinate P^{III} compounds (e.g., phosphaalkenes, iminophosphines, phosphenium salts). Examples of reactions that illustrate the need for robust and nonreactive counteranions for the systematic study of the chemistry of P^I cations, such as ligand replacement chemistry,[52] will be detailed in future publications.

Each of the salts formed by the anion exchange reactions was characterized completely by multinuclear NMR and other suitable analytical methods; in the cases of the tetraphenylborate, triflate, hexafluorophosphate, and tetrachlorogallate salts, crystals suitable for examination using X-ray crystallography were also obtained by recrystallization from either acetonitrile or dichloromethane.

The tetraphenylborate salt **4**[BPh_4] crystallizes in the space group $P2_1/c$; the molecular structure is depicted in Figure 4, and pertinent metrical parameters are assembled in Table 2. The solid-state arrangement of the salt consists of discrete cations and anions, and there are no unusually short contacts between any of the ions. The metrical parameters for the anion correspond to those anticipated for an undistorted tetraphenylborate anion, and the metrical parameters for the cation are entirely consistent with those found in **4**[I].

Crystals of suitable quality for analysis by single-crystal X-ray diffraction were likewise obtained for the tetraphenylborate salt **5**[BPh_4], which crystallizes in the space group $P2_1/c$. The molecular structure is depicted in Figure 5, and relevant metrical parameters are compiled in Table 2. Once again there are no unusually close contacts between the cation and anion. The metrical parameters of the tetraphenylborate

(49) Kirsanov, A. V.; Gorbatenko, Z. K.; Feshchenko, N. G. *Pure Appl. Chem.* **1975**, *44*, 125−139.

(50) Preliminary results suggest that $(PI)_n$ is the primary component of the insoluble orange precipitate formed in these reactions. Further investigations to elucidate the structure and reactivity of this material are currently underway.

(51) Baudler, M.; Grenz, D.; Arndt, U.; Budzikiewicz, H.; Feher, M. *Chem. Ber.* **1988**, *121*, 1707−1709.

(52) Ellis, B. D.; Dyker, C. A.; Decken, A.; Macdonald, C. L. B. *Chem. Commun.* **2005**, 1965−1967.

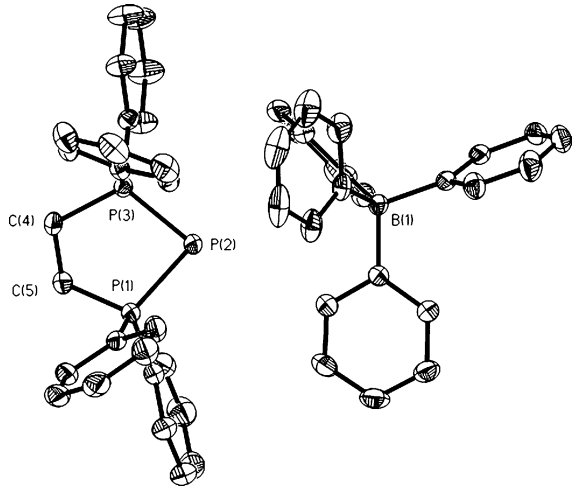

Figure 4. Thermal ellipsoid plot (30% probability surface) of **4**[BPh_4]. H atoms are omitted for clarity.

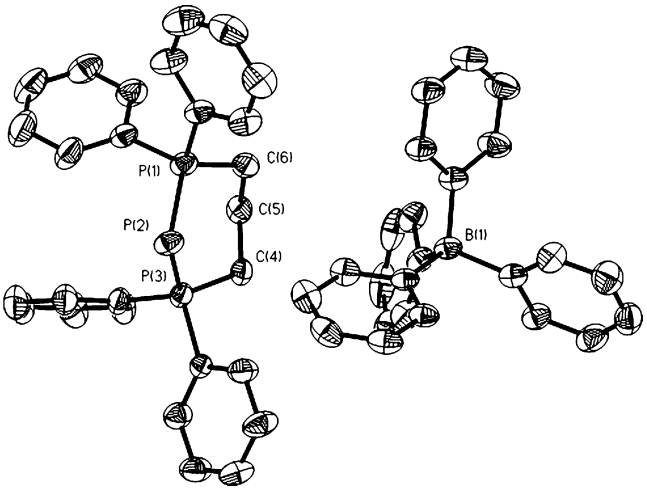

Figure 5. Thermal ellipsoid plot (30% probability surface) of **5**[BPh_4]. H atoms are omitted for clarity.

anion are consistent with those expected, and those of the cation are similar to those observed in the structure of **5**[I].

In a similar manner, the tetrachlorogallate and hexafluorophosphate salts of **5**, **5**[$GaCl_4$], and **5**[PF_6] also gave crystals suitable for crystallographic analysis. Both salts crystallized in the monoclinic space group $P2_1/c$. Figures 6 and 7 show the molecular structures, and pertinent metrical parameters are summarized in Table 2. The anions in both salts exhibit metrical parameters that are unexceptional and that do not suggest any strong interactions with the cations; the cations are again consistent with those observed in the iodide and tetraphenylborate salts described above. The salt **5**[PF_6] is also interesting in that it is an example of a single compound containing P atoms in two-, four-, and six-coordinate environments.

Theoretical Results and Predictions. In an effort to explain the remarkable stability of the univalent P cations that we have examined experimentally, we performed a series of DFT calculations. To assess the importance of the nature of the donor ligands on the stabilities of the complexes, the model compounds were chosen to contain either phosphine [PH_3, **7**; PMe_3, **8**; dhpe = 1,2-bis(phosphino)ethane, **9**; dmpe = 1,2-bis(dimethylphosphino)ethane, **10**], amine (NH_3, **11**; NMe_3, **12**; en = ethylenediamine, **13**; tmeda = tetramethylethylenediamine, **14**), or both phosphine and amine (PH_3/NH_3, **15**; PMe_3/NMe_3, **16**; $H_2P(CH_2)_2NH_2$, **17**; $Me_2P(CH_2)_2$-NMe_2, **18**) donor groups to the P^I center. For completeness, these model compounds include both acyclic and cyclic examples and are depicted in Figure 8. A summary of important calculated values is presented in Table 3.

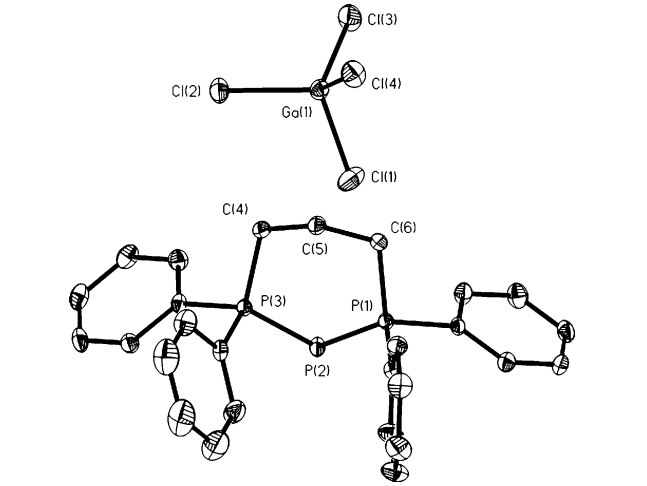

Figure 6. Thermal ellipsoid plot (30% probability surface) of **5**[$GaCl_4$]. H atoms are omitted for clarity.

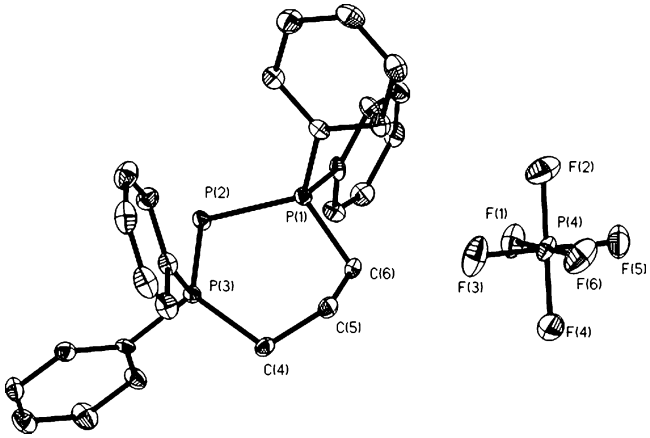

Figure 7. Thermal ellipsoid plot (30% probability surface) of **5**[PF_6]. H atoms are omitted for clarity.

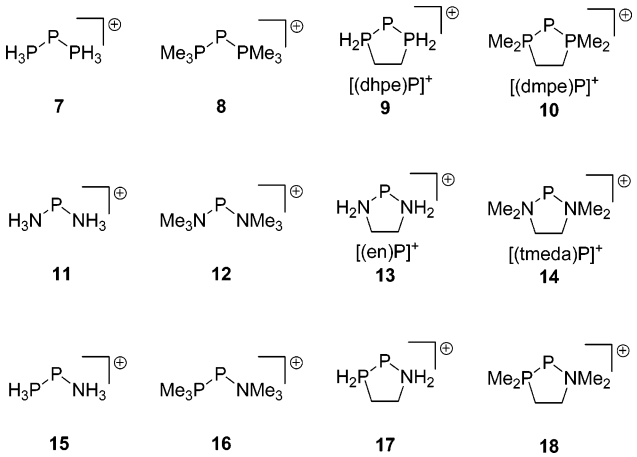

Figure 8. Model cation systems **7**−**18** investigated using DFT methods.

Table 3. Summary of Computational Results for Compounds **7**−**18**

model	sym	corrected energy, E_{total}[a] (au)	E_{HOMO} (eV)	E_{LUMO} (eV)	P−P (Å)	P−N (Å)	E−P−E (deg)	occ P[b] (3p)	q(P)[c] (au)	P−P WBI[d]	P−N WBI[d]	P−P BO[e]	P−N BO[e]	P(3p) (%)[f]
7	C_{2v}	−1027.159 94	−10.852	−5.919	2.153		97.0	1.721	−0.22	1.0979		0.8328		86.398
8	C_{2v}	−1262.911 80	−9.342	−4.126	2.150		105.0	1.729	−0.32	1.0971		0.8166		85.976
9	C_2	−1104.550 33	−10.405	−5.775	2.152		87.8	1.673	−0.22	1.1014		0.8579		83.949
10	C_2	−1261.723 64	−9.406	−4.207	2.149		90.2	1.664	−0.27	1.1070		0.9031		83.328
11	C_{2v}	−454.013 14	−9.700	−5.787		1.925	93.9	1.947	0.31		0.6274		0.4947	97.535
12	C_2	−689.625 46	−8.746	−4.231		1.944	107.3	1.938	0.30		0.5836		0.4483	96.993
13	C_2	−531.371 69	−9.352	−5.530		1.931	86.3	1.948	0.30		0.6106		0.4760	97.578
14	C_2	−688.450 28	−8.748	−4.809		1.926	90.6	1.924	0.33		0.5877		0.4693	96.318
15	C_s	−740.586 20	−10.404	−6.376	2.142	1.934	97.2	1.789	0.08	1.1438	0.6433	0.8556	0.4878	89.736
16	C_1	−976.267 98	−9.097	−4.837	2.151	1.930	105.9	1.800	0.02	1.1311	0.6027	0.8034	0.4855	90.046
17	C_1	−817.959 86	−10.014	−5.894	2.142	1.934	87.1	1.725	0.08	1.1296	0.6330	0.8601	0.4770	88.740
18	C_1	−975.084 67	−9.160	−4.968	2.144	1.935	90.2	1.764	0.06	1.1339	0.6041	0.9032	0.4660	87.596

[a] $E_{total} = E_{calcd}$ + ZPVE. [b] NBO population of the $3p_x$ orbital on the dicoordinate P atom. [c] NBO charge on the dicoordinate P atom. [d] NBO Wiberg bond indices for the specified bonds. [e] NBO atom−atom overlap-weighted natural atomic orbital bond order for the specified bonds. [f] NBO NLMO percentage contribution of the $3p_x$ orbital on the dicoordinate P atom to the "lone-pair" or delocalized "lone-pair" orbital.

The calculated metrical parameters in models **7**−**10** are in reasonably good agreement with those that have been determined experimentally given the simplified nature of the models and attest to the viability of the chosen models. Although the calculated P−P distances tend to be slightly longer than those observed in the crystallographic experiments outlined above, the values are still much shorter than those of typical single P−P bonds.[53] In contrast, the models employing amine substitutents (**11**−**14**) have computed bond lengths that are much longer than typical P−N single bonds [cf. 1.800(4) Å for O_3PNH_3[54] and 1.696(3) Å for PhHN−PPh_2[55]]. Although such long P−N distances may appear odd, it must be emphasized that the covalent radius of P^I will be significantly larger than those of P^{III} or P^V, which are contained in the compounds containing the "typical" bonds. The model compounds containing both phosphine and amine donors (**15**−**18**) exhibit calculated P−P and P−N bond lengths that are comparable to those of the corresponding homoleptic models. The calculated P−P−P angles for the cyclic models **9** and **10** correlate well with those observed experimentally for salts of **4**. Similarly, the calculated angles for the acyclic triphosphenium cations **7** and **8** are also in good agreement with reported experimental values.[37]

The potentially ambiguous nature of the electronic structure of triphosphenium cations is emphasized by the possible canonical drawings that may be used to depict such compounds, as illustrated by structures **1a**−**d**. Drawing **1a** suggests the presence of a P^V center bearing no "lone pairs" of electrons and exhibiting a linear, allene-like P═P═P geometry. Because every structurally characterized triphosphenium compound has a strongly bent P−P−P moiety, drawing **1a** is not an instructive or reasonable depiction of such cations. Accordingly, if computational models such as **7** are constrained to D_{3d} symmetry, they exhibit several imaginary frequencies and are thus not true minima on their potential energy surfaces. In the literature, triphosphenium cations are most typically depicted using drawings such as **1b**, in which the dicoordinate P atom has one "lone pair" of electrons and is thus a P^{III} center. Model **1b** also suggests the presence of one double bond delocalized between the dicoordinate P center and the P atoms of the phosphine substituents and could thus account for the short P−P distances observed experimentally. A third Lewis-type structure that is sometimes used to depict triphosphenium cations is a bis-ylidic model illustrated by **1c**, in which the dicoordinate P atom bears two "lone pairs" of electrons and is thus able to be described as a P^I center. An alternative but equivalent depiction of **1c** is **1d**, which may be used to emphasize that such molecules can be considered as coordination compounds of P^I cations.

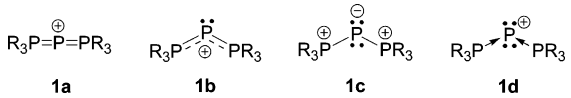

1a **1b** **1c** **1d**

While Lewis-type drawings should certainly not be overinterpreted, such simple models can provide insight into the structural properties and potential reactivity of compounds such as **1**. In this vein, we examined the frontier orbitals of model compounds **7**−**18** in an effort to gain insight into the real electronic structure of triphosphenium cations and to assess the appropriateness of models such as **1b** and **1c**. Drawings of the relevant frontier orbitals for the most realistic cyclic models **10**, **14**, and **18** are presented in Figure 9, and pertinent details of the NBO analysis are listed in Table 3.

Perhaps the most important overall feature that is apparent in Figure 9 is the general similarity of the appearance of two highest occupied molecular orbitals (HOMO-1 and HOMO) in each model regardless of the composition of the stabilizing ligand. In every case, the HOMO-1 orbital is of *a*-type symmetry and is consistent with a "lone pair" orbital on the dicoordinate P atom in the E−P−E plane (where E = N or P depending on the model). Similarly, the HOMO in each of the models is a *b*-type symmetry (for the C_2 models) orbital that is almost exclusively composed of the atomic $3p_x$ orbital on the dicoordinate P atom. The HOMOs

(53) Hinchley, S. L.; Morrison, C. A.; Rankin, D. W.; Macdonald, C. L.; Wiacek, R. J.; Voigt, A.; Cowley, A. H.; Lappert, M. F.; Gundersen, G.; Clyburne, J. A.; Power, P. P. *J. Am. Chem. Soc.* **2001**, *123*, 9045−9053.
(54) Cameron, T. S.; Chan, C.; Chute, W. J. *Acta Crystallogr., Sect. B: Struct. Crystallogr. Cryst. Sci.* **1980**, *B36*, 2391−2393.
(55) Wetzel, T. G.; Dehnen, S.; Roesky, P. W. *Angew. Chem., Int. Ed.* **1999**, *38*, 1086−1088.
(56) Schaftenaar, G.; Noordik, J. H. *J. Comput.-Aided Mol. Des.* **2000**, *14*, 123−134.

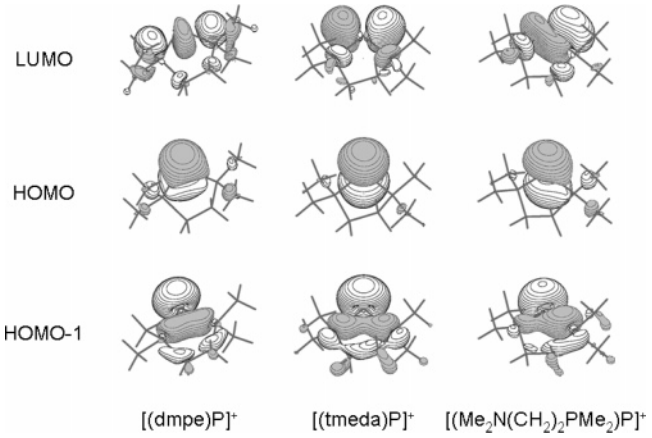

Figure 9. MOLDEN[56] depictions of the HOMOs and LUMOs for the model cations **10**, **14**, and **18**.

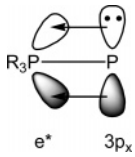

Figure 10. Orbital interactions between the empty P−R anti-bonding orbitals and a filled $3p_x$ orbital on P^I allowing for back-bonding from the dicoordinate P^I to the phosphine substituents.

thus appear almost identical with those of water and suggest that the ylidic model **1c** (or **1d**) is the most appropriate drawing in terms of the overall electronic structure.

Despite the general similarity in the appearance of the occupied orbitals of the model compounds depicted in Figure 9 and those of the other model compounds listed in Table 3, there are significant differences between them in terms of their energies. In particular, whereas the energy of the lowest unoccupied MO (LUMO) remains roughly similar in the corresponding models regardless of whether they contain amine or phosphine ligands, the energies of the HOMOs are considerably lower for models containing phosphine ligands. For example, in the series of models **9**, **13**, and **17**, the energies of the LUMOs are similar: −5.775, −5.530, and −5.894 eV, respectively. In sharp contrast, the energies of the corresponding HOMOs are significantly different, with the values being −10.405, −9.352, and −10.014, respectively. Thus, it is apparent that the presence of phosphine donor ligands on the dicoordinate P center stabilizes the HOMO and increases the HOMO−LUMO separation in comparison to when amine donors are used.

Given the foregoing, an explanation for the remarkable stability of triphosphenium cations is almost certainly related to the stabilization of the HOMO. An explanation is provided by the understanding that, in contrast to amines, phosphine ligands may act as back-bonding acceptors, as they are known to do in compounds containing phosphines ligated to transition metals. In phosphine ligands, the empty π-type P−R antibonding orbitals (these have *e* symmetry in the C_{3v} point group of the free PR_3 ligand) are of the correct symmetry and appropriate energy to accept electron density from the filled $3p_x$ orbital on the P^I center (Figure 10). Such a back-bonding interaction lowers the energy of the MO thus formed and stabilizes the electron-rich center. It should be noted that, in main group or organic compounds, back-bonding interactions of the type depicted in Figure 10 are more commonly described using the term "hyperconjugation".

Direct evidence for the presence of back-bonding interactions is found in the results of the NBO population analysis. In the absence of a back-bonding interaction, the population of the $3p_x$ orbital on the P^I center should be roughly two electrons. In all of the models containing phosphine ligands, back-bonding allows for the effective partial oxidation of the P^I center, which is reflected in the decreased population of the $3p_x$ orbital on the dicoordinate P center, as shown in Table 3. A comparable decrease in the $3p_x$ population is not observed in the case of the models containing the corresponding amine ligands in which the orbital population remains at a value of almost 2. The magnitude of the interaction is also confirmed by the results of natural localized MO (NLMO) calculations, which provide a measure of the delocalization of the "lone pair" orbitals. As listed in Table 3, these calculations show virtually no delocalization in the amine-substituted models and significant delocalization in the phosphine-containing models. Furthermore, the NBO analysis indicates that the back-bonding delocalization stabilizes the model compound $[(H_3P)_2P]^+$ **7** by around 187 kJ mol^{-1}, while the much-less-favorable interaction in the model $[(H_3N)_2P]^+$ **11** provides only 66 kJ mol^{-1} of stabilization. For the cations containing both phosphine and amine substituents, there is a decrease in the orbital population, although less than that observed for models containing two phosphine donors.

In addition to the differences in orbital occupancies and energies, the presence or absence of the back-bonding interaction is clearly manifested in the shape of the HOMO for each of the model cations, as depicted in Figure 9. In the case of models containing phosphine ligands, there are perturbations of the lobe derived primarily from the $3p_x$ orbital on the P^I center toward the phosphine substituents to produce orbitals that are consistent with the presence of a π-bonding interaction between the P atoms. The much smaller magnitude of the back-bonding in the amine-substituted models is further emphasized by the presence of a nearly undistorted $3p_x$ orbital on P^I in the HOMO of the model depicted in Figure 9.

In addition to the effects on the shape and composition of the HOMO, the greater magnitude of back-bonding in the phosphine-substituted model compound $[(H_3P)_2P]^+$ (**7**) is highlighted by the structural consequences of preventing the back-bonding interactions. When the important acceptor orbitals on the phosphine ligands are removed using the NBOdel method, the optimized P−P bond distance increases to 2.350 Å from the 2.149 Å distance in the unperturbed model; this is a change of more than 0.2 Å. The comparable change in the amine-substituted analogue is less than 0.1 Å (from 1.919 to 2.012 Å). For the mixed-ligand model system $[(H_3P)P(NH_3)]^+$ (**15**), the P−P bond distance changes from 2.141 to 2.364 Å, while the P−N bond distance only changes from 1.926 to 2.022 Å when back-bonding interactions are prevented. Thus, both structural features and energy values

demonstrate that the magnitude of the back-bonding is clearly more pronounced for the phosphine ligands, as one would expect. In this light, the Lewis-type model **1b** certainly provides insight into the stability of triphosphenium cations.

In addition to the effects on the occupied orbitals, it is notable that the composition of the LUMO is also highly dependent on the nature of the ligands, as shown in Figure 9. For model **10**, the LUMO is localized primarily on the phosphine substituents, whereas for **14**, the orbital is principally on the dicoordinate P atom (the MO resembles a $3p_y$ atomic orbital) and, for **18**, the orbital is mainly localized over the two P atoms. Thus, the calculations suggest that the nature of the ligand not only affects the stability of the E−P−E framework but also should have a large impact on the reactivity of the coordinated P^I center. Overall, these computational results suggest that there are many possible ways to tune the reactivity of such compounds through the judicious choice of stabilizing ligand. While there is much more experimental work to be done in this regard, we have already demonstrated that an understanding of the frontier MOs can be used to control the oxidation chemistry of some analogous As^I compounds.[47]

Overall, examinations of the electronic structure of several model compounds suggest that the two HOMOs in triphosphenium cations correspond to "lone pairs" of electrons that are primarily localized on the dicoordinate P atom; in this light, the ylidic description (**1c**) of the bonding in such molecules is the most appropriate. However, the HOMO in triphosphenium cations is rendered significantly more stable by back-bonding interactions with the adjacent phosphine ligands so, while ylidic depictions such as **1c** most accurately describe the electronic structure, a canonical structure such as **1b** provides insight into the remarkable stability of these compounds.

Conclusions

High-purity iodide salts of cations containing P^I centers are readily prepared and isolated in good yield by the base-induced spontaneous elimination of I_2 from PI_3. The facile exchange of the I^- anion in **4**[I] or **5**[I] using metathesis reactions allows for the tailoring of reactivity and solubility of univalent P salts and will allow for further investigations into the unique chemistry and potential uses for this easily accessible reagent. In contrast to most other P^I compounds, many of these salts are stable even in the presence of water and air. The remarkable stability of these P^I salts is largely attributable to the back-bonding interactions between the ligand and the P^I center, and such an understanding may be used to tune the behavior of these reagents.

Acknowledgment. We thank the Natural Sciences and Engineering Research Council (NSERC, Canada), the Canada Foundation for Innovation, the Ontario Research and Development Challenge Fund, and the Ontario Innovation Trust for financial support. B.D.E. thanks the Government of Ontario and NSERC for postgraduate scholarships. We also thank Michelle Carlesimo and Kevin A. Renaud for some synthetic work, the CCMR (Windsor) for elemental analyses, and Dr. R. J. Letcher's laboratory (GLIER) and Dr. J. R. Green (Windsor) for obtaining the mass spectra.

Supporting Information Available: X-ray crystallographic data in CIF format for compounds **4**[I], **4**[BPh_4], **5**[I], **5**[BPh_4], **5**[OTf], **5**[BF_4/I], **5**[PF_6], **5**[$GaCl_4$], and **6** are provided. Cartesian coordinates for the geometry optimizations and a summary of calculation results are tabulated. This material is available free of charge via the Internet at http://pubs.acs.org.

IC060186O